

Supporting Information

A Quartz Crystal Microbalance Method to Study the Terminal Functionalization of Glycosaminoglycans

Dhruv Thakar, Elisa Migliorini, Liliane Coche-Guerente, Rabia Sadir, Hugues Lortat-Jacob, Didier Boturyn, Olivier Renaudet, Pierre Labbe, and Ralf P. Richter*

Table of Contents

Supplementary Materials and Methods	S2
Synthesis of b-OEG-ONH ₂ 5	S3
Supplementary Figures	S6
Supplementary References	S12

Supplementary Materials and Methods

GAGs and proteins

HS with an average molecular weight of 12 kDa and a polydispersity of 1.59,¹ derived from porcine intestinal mucosa, was obtained from Celsus Laboratories (Cincinnati, Ohio). HS oligosaccharides (HS_dp6, HS_dp8, HS_dp10, HS_dp12) presenting GlcNAc at their reducing end were prepared as previously described.² HA oligosaccharides (HA_dp4, HA_dp10) presenting GlcNAc at their reducing end were purchased from Hyalose (Oklahoma, OK, USA). Lyophilized streptavidin (SAv) and bovine serum albumin (BSA) were purchased from Sigma-Aldrich (Saint-Quentin Fallavier, France), suspended in autoclaved Hepes buffer (10 mM Hepes (Fisher, Illkirch, France), pH 7.4, 150 mM NaCl (Sigma-Aldrich)) and stored at -20°C.

An oligonucleotide (⁵X AAT TCG CTA GCT GGA GCT TGG ATT GAT GTG GTG TGT GAG TGC GGT GCC C³, X represents the 5' amino linker; $M_w = 15\,440$ Da) and an equivalent oligonucleotide with a biotin (⁵AAT TCG CTA GCT GGA GCT TGG ATT GAT GTG GTG TGT GAG TGC GGT GCC C X³, X represents the 3' biotin tetraethyleneglycol linker; $M_w = 15595.3$ Da) were synthesized at 0.2 μmol scale using standard β -cyanoethyl phosphoramidite chemistry on a DNA synthesizer (ABI 3400). After elongation, oligonucleotides were cleaved from the solid support and released into solution by treatment with 28% ammonia (1.5 mL) for 2 h and finally deprotected by keeping in ammonia solution for 16 h at 55 °C. Purifications were carried out by denaturing polyacrylamide gel electrophoresis and oligonucleotides were desalted by SEC on NAP-10 columns (GE Healthcare, Velizy-Villacoublay, France). Quantifications were performed at 260 nm using a CARY 400 Scan UV-Visible Spectrometer (L-tym: 16 nmoles, 13 %, $\epsilon_{260\text{nm}} = 463600 \text{ M}^{-1}\text{cm}^{-1}$); ϵ was estimated according to the nearest neighbour model.

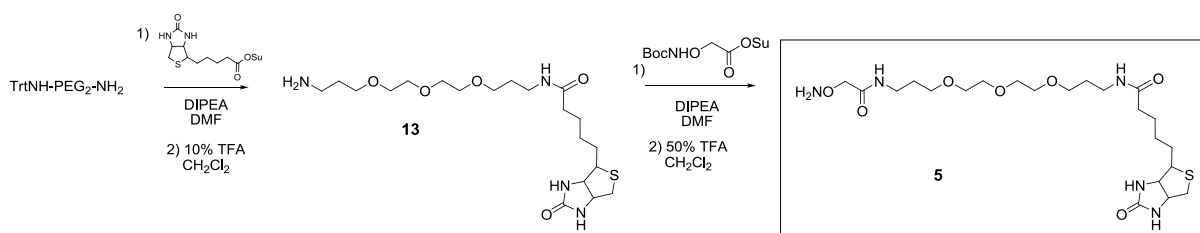
Biotinylation of GAGs

For oxime ligation, the GAGs (4 mM) were suspended in 100 mM acetate buffer, made from glacial acetic acid (Fisher, Illkirch, France) and sodium acetate (Sigma-Aldrich), at pH 4.5. They were then reacted with b-OEG-ONH₂ 5 (3.4 mM; synthesized as described on page S3) in the presence of aniline (100 mM; Sigma-Aldrich) for 48 h at 37°C. Hydrazone ligation was performed as previously described.³ Briefly, HS suspended in phosphate-buffered saline (PBS; Sigma Aldrich), pH 7.4 at 0.33 mM was reacted for 48 h at room temperature with 10 mM biotin-LC-hydrazine (Pierce, Rockford, USA). The final mixtures for both reactions were purified either by extensively dialyzing against water through membranes with a molecular weight cutoff (MWCO) of 1000 Da (Spectra/Por, France) or by using a desalting column (Pd-10 G-25M with MWCO = 5000 Da; GE Healthcare), depending on the molecular weights used, to remove unreacted biotin and aniline. The final products, typically containing a mixture of unreacted and biotin-conjugated GAGs, were then lyophilized and stored at -20°C, either as is or re-solubilized in Hepes buffer or ultrapure water at a concentration of 10 mg/mL. Under these storage conditions, none of the samples was found to degrade appreciably. For further use, the conjugates were diluted to desired concentrations in Hepes buffer.

Quartz crystal microbalance with dissipation monitoring (QCM-D)

QCM-D measures the changes in resonance frequency, Δf , and dissipation, ΔD , of a sensor crystal upon molecular binding events on its surface. The QCM-D response is sensitive to the mass (including hydrodynamically coupled water) and the mechanical properties of the surface-bound layer. Measurements were performed with a Q-Sense E4 system equipped with 4 independent Flow Modules (Biolin Scientific, Västra Frölunda, Sweden). Before use, the walls of the liquid handling system were passivated against biomolecular binding with bovine serum albumin (BSA). The system was operated in flow mode with a flow rate of typically 10 $\mu\text{L}/\text{min}$ using a peristaltic pump (ISM935C, Ismatec, Zurich, Switzerland). The working temperature was 24°C. Δf and ΔD were measured at six overtones ($n = 3, 5, \dots, 13$), corresponding to resonance frequencies of $f_n \approx 5, 15, 25, \dots, 65$ MHz; changes in dissipation and normalized frequency, $\Delta f = \Delta f_n/n$, of the third overtone ($n = 3$) are presented. Any other overtone would have provided comparable information.

Synthesis of b-OEG-ONH₂ 5



Scheme Syn1. Steps for the synthesis of the bi-functional linker b-OEG-ONH₂ 5, presenting a biotin and an oxyamine moiety (–ONH₂).

The synthesis route is schematically shown in Scheme Syn1. Unless otherwise stated, chemical reagents were purchased from Sigma Aldrich (Saint Quentin Fallavier, France) or Acros (Noisy-Le-Grand, France) and were used without further purification. Analytical RP-HPLC was performed on a Waters system equipped with a Waters 600 controller and a Waters 2487 Dual Absorbance Detector. Analysis was carried out at 1.0 mL/min (EC 125/3 nucleosil 300-5 C₁₈) with UV monitoring at 214 nm and 250 nm using a linear A–B gradient (buffer A: 0.09% CF₃CO₂H in water; buffer B: 0.09% CF₃CO₂H in 90% acetonitrile). Preparative separation was carried out at 22 mL/min (VP 250/21 nucleosil 300-7 C₁₈) with UV monitoring at 214 nm and 250 nm using a linear A–B gradient (buffer A: 0.09% CF₃CO₂H in water; buffer B: 0.09% CF₃CO₂H in 90% acetonitrile). Mass spectrometry was performed using electrospray ionization on an Esquire 3000+ Bruker Daltonics in positive mode. ¹H NMR spectra were recorded in D₂O at 400 MHz with a Bruker Avance 400 spectrometer.

Synthesis of compound 13. TrtNH-PEG₂-NH₂ (200 mg, 0.43 mmol; Calbiochem-Novabiochem (Merck Biosciences - VWR, Limonest, France)) and biotin-OSu (220 mg, 0.65 mmol; Calbiochem-Novabiochem) were dissolved in dry DMF (10 mL) containing DIPEA (75 μL, 0.43 mmol) and the solution was stirred at room temperature. After 45 min RP-HPLC analysis indicated complete reaction (*R_t* = 12.29 min, 5-100% B in 20 min). The solvent was then evaporated under reduced pressure and the crude oily residue was taken up with a solution of 10% TFA in CH₂Cl₂ (10 mL) containing 0.1% of triisopropylsilane. The solution was evaporated after 1 h and diethyl ether was added to precipitate compound 13 which was obtained as a white powder after centrifugation. Yield: 77% (149 mg); *R_t* = 7.97 min (5-100% B in 20 min); ESI-MS: *m/z* calcd. for C₂₀H₃₉N₄O₅S (M + H)⁺ 447.3, found 447.5.

Synthesis of compound 5. Compound 13 (50 mg, 0.11 mmol) was dissolved in dry DMF (5 mL) containing DIPEA (19.5 μL, 0.11 mmol). Boc-Aoa-OSu (39 mg, 0.13 mmol) was added to the solution and the mixture was stirred at room temperature until complete disappearance of the starting material observed by analytical HPLC (*R_t* = 10.17 min, 5-100% B in 20 min). The solvent was removed and the residue was precipitated in diethyl ether. The resulting white powder was next stirred 30 min at room temperature in 50% TFA in CH₂Cl₂ (5 mL). After solvent evaporation, the crude mixture was purified by preparative RP-HPLC to afford compound 5 (Fig. Syn1). Yield: 74% (43 mg); *R_t* = 7.96 min (5-100% B in 20 min); ESI-MS (Fig. Syn2): *m/z* calcd. for C₂₂H₄₂N₅O₇S (M + H)⁺ 520.3, found 520.5.

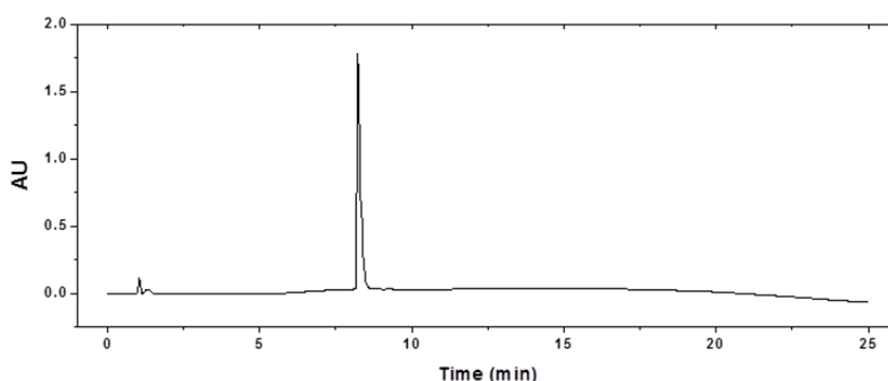


Figure Syn1. Crude RP-HPLC profile (5 to 100% B in 100 min, λ = 214 nm) of compound 5.

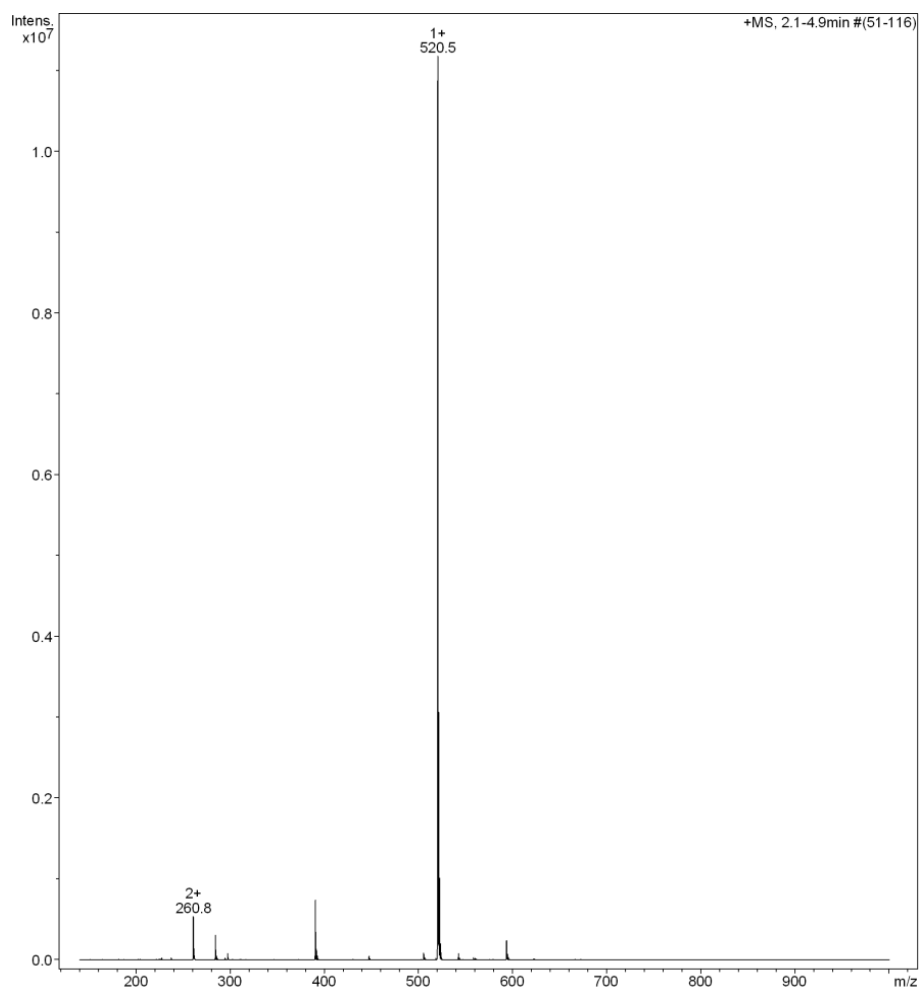


Figure Syn2. ESI-MS (positive mode) of compound **5**.

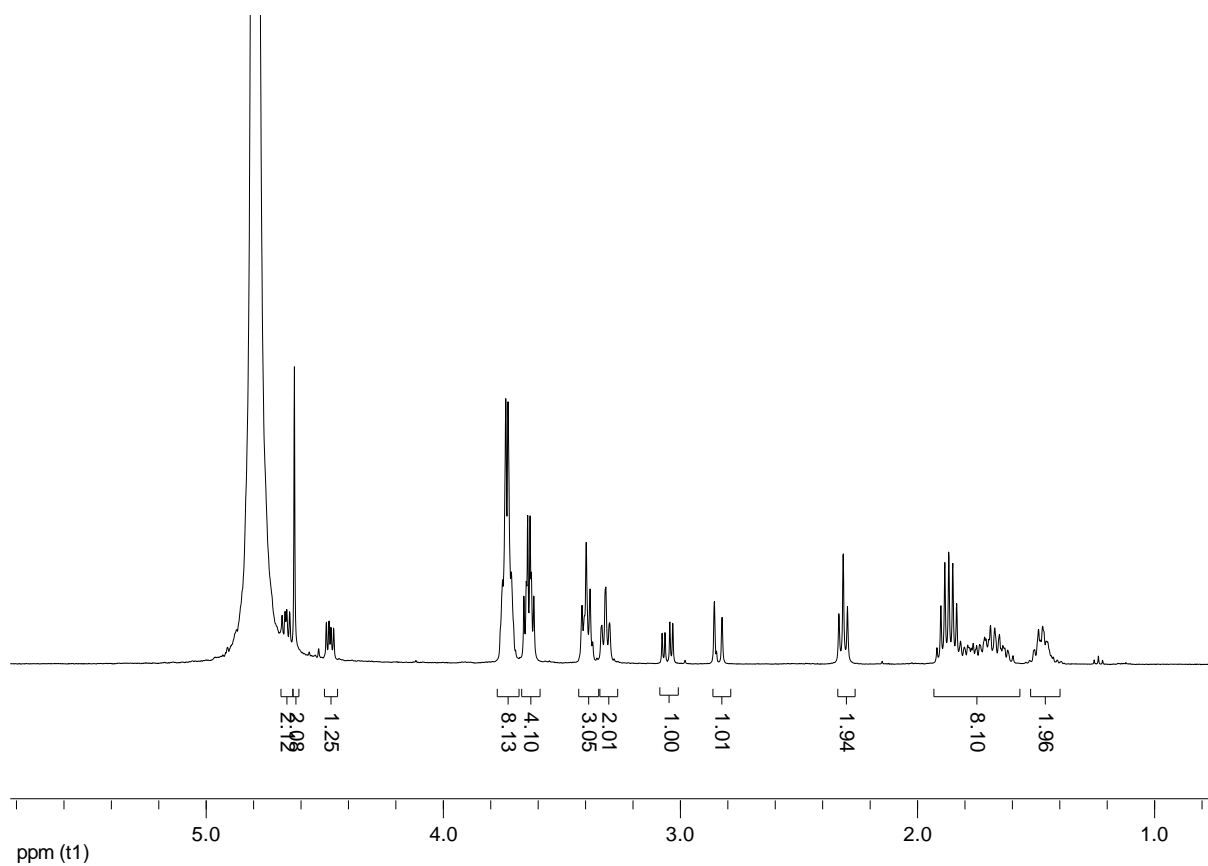


Figure Syn3. ¹H NMR spectrum (400 MHz, D₂O) of compound 5.

Supplementary Figures

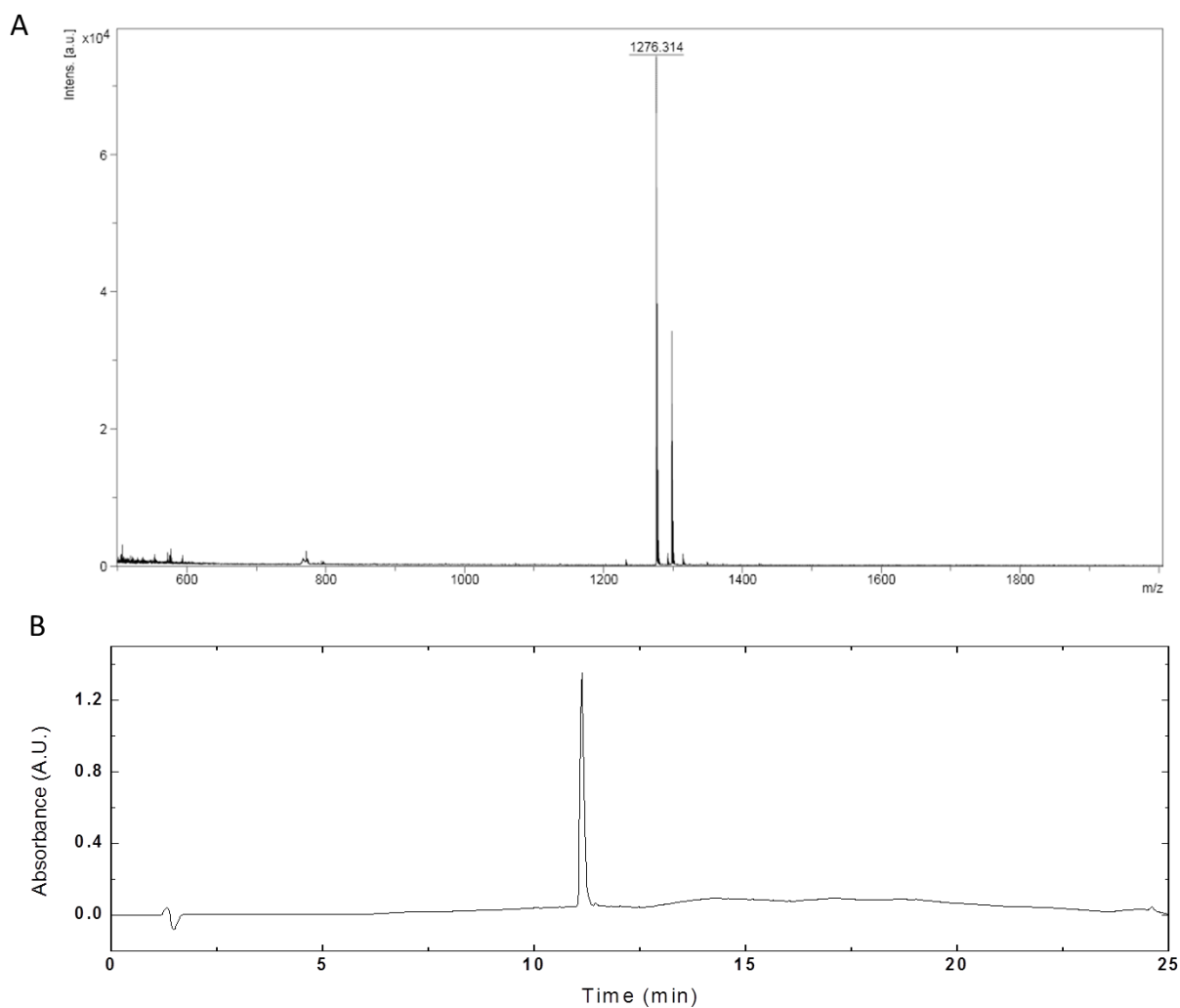


Figure S1. Analysis of biotinylated HA_dp4. (A) Mass spectrum (ESI-MS, negative mode) of biotinylated HA_dp4 (b-HA_dp4 **10**), m/z calcd for $C_{50}H_{83}N_7O_{29}S$: 1278.3; found m/z : 1277.3, the peak at 1298.3 corresponds to $[M+Na-H]^-$. This confirms the attachment of one biotin group per HA chain. (B) HPLC Chromatogram (5 to 100% B in 100 min, $\lambda = 214$ nm) of **10**. The peak at 11.1 min corresponds to the final product. HA_dp4 (1.4 mg, 1.8 μ mol) was mixed with b-OEG-ONH₂ **5** (3.4 mM) and aniline (100 mM) in acetate buffer (100 mM), pH 4.5, 37°C for 48 h. The reaction mixture was purified using HPLC to obtain **10** (1.3 mg, 1.0 μ mol, yield = 56%) as a white powder after freeze-drying.

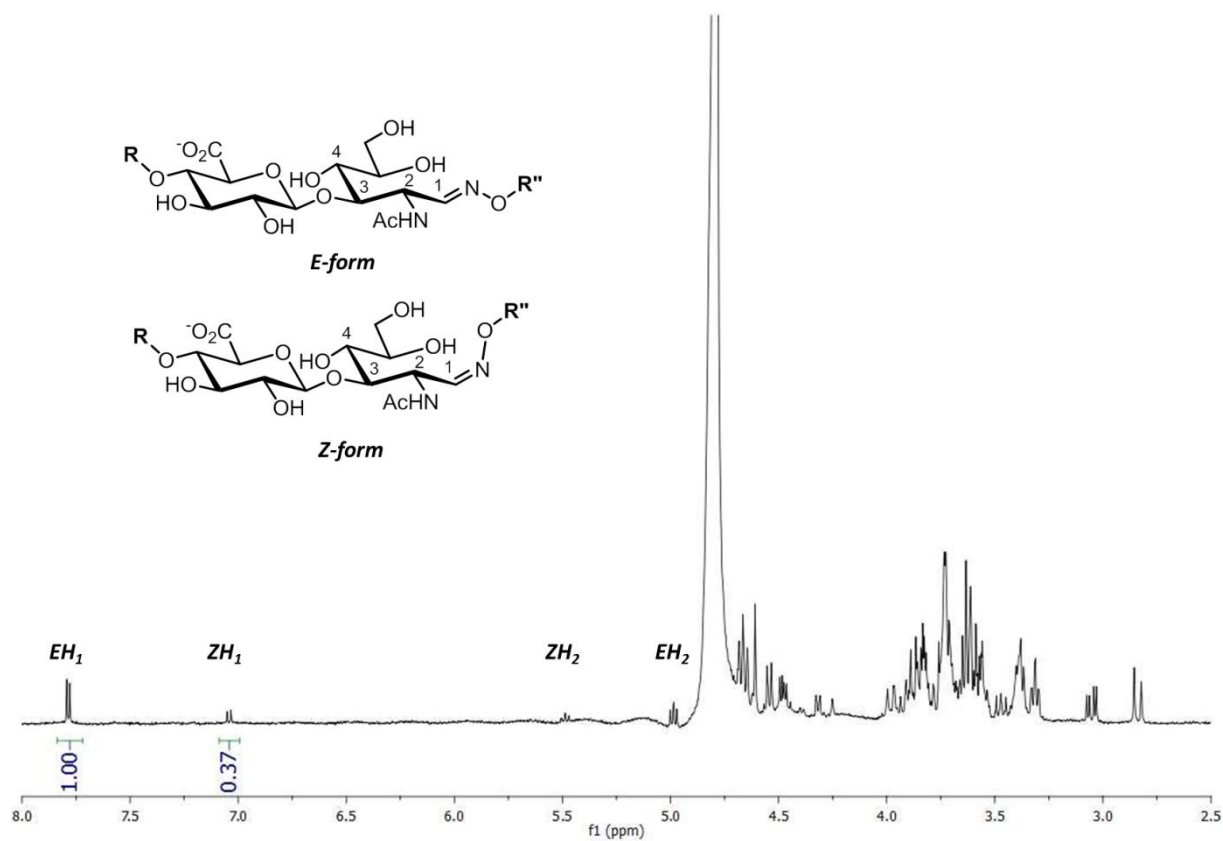


Figure S2. NMR analysis of **b-HA_dp4 10**. The ¹NMR analysis shows the formation of E and Z conformations of **10**, indicating that the attachment of biotin occurs at the reducing end of HA which leads to both the open and closed forms. Integrating the signals corresponding to the two conformations, the oxime link was found to be 73% and 27% in E and Z conformation, respectively. R is a GlcA β(1→3) GlcNAc β(1→4) disaccharide, and R'' is defined in Scheme 1.

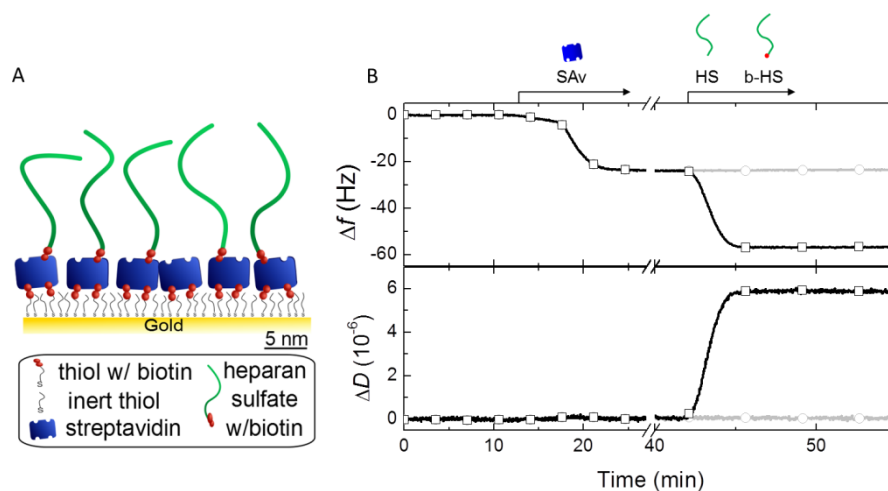


Figure S3. QCM-D binding assay. (A) Schematic presentation of the streptavidin (SAv)-presenting surface used to study the yield and stability of GAG biotinylation. (B) Representative QCM-D binding assay with frequency shifts, Δf , and dissipation shifts, ΔD . Prior to each QCM-D measurement, QCM-D sensors with a new gold coating (QX301, Biolin Scientific) were cleaned by rinsing with ultrapure water, blow-drying with N_2 and exposure to UV/ozone (Jelight, Irvine, CA, USA) for 10 min; within 5 min after UV/ozone treatment, the sensors were immersed in an ethanolic solution (Fisher) of oligo ethyleneglycol (OEG) disulfide and biotinylated OEG thiol (Polypure Oslo, Norway), at a total concentration of 1 mM and a molar ratio of thiol equivalents of 999:1; after overnight incubation, the sensor surfaces were rinsed with ethanol and blow-dried with N_2 , before being installed in the QCM-D modules. Start and duration of sample incubation steps are indicated by arrows on top of the plot; during remaining times, the surface was exposed to Hepes buffer solution. SAv was initially incubated at a concentration of 1 $\mu\text{g}/\text{mL}$ at a small flow rate (6 $\mu\text{L}/\text{min}$) for 4 min, and then at 20 $\mu\text{g}/\text{mL}$ at standard flow rate (10 $\mu\text{L}/\text{min}$). At equilibrium, SAv generated frequency shifts $\Delta f = -23 \pm 1$ Hz and dissipation shifts $\Delta D < 0.4 \times 10^{-6}$ which are characteristic for the formation of a dense protein monolayer. The injection at low concentration was routinely performed to confirm the absence of protein depletion resulting from undesired adsorption to the walls of the tubing or the QCM-D flow module due to insufficient passivation: any depletion of SAv from the solution would result in a decreased binding rate. GAGs were incubated at 50 $\mu\text{g}/\text{mL}$. End-biotinylated HS (b-HS_12kDa **3** (oxime), black lines with square symbols) readily bound to the free biotin-binding sites on the SAv monolayers. The ensuing shift in frequency and the strong increase in dissipation indicate the formation of a soft and hydrated layer as would be expected for a film of end-grafted HS chains. Biotin-free GAGs (grey lines with circle symbols) showed no response, confirming that the immobilization of GAGs on the SAv monolayer occurs exclusively through the biotin moiety at the GAG's reducing end.

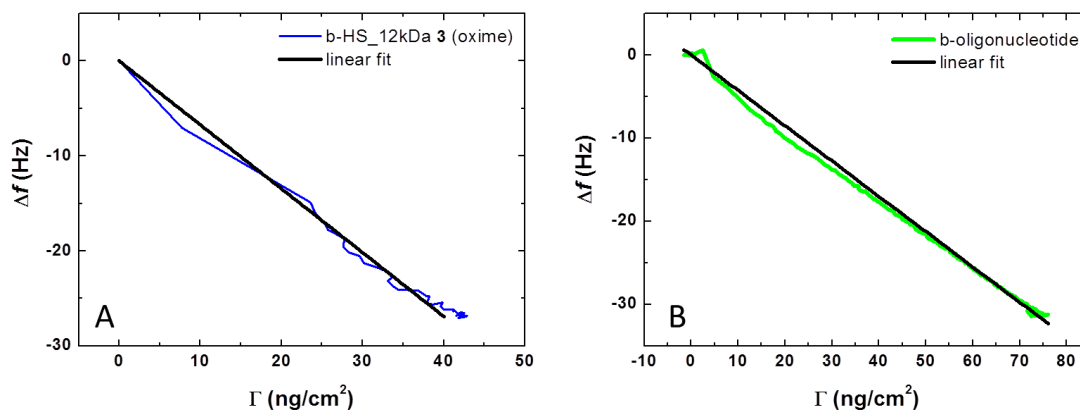


Figure S4. Relationship between the QCM-D frequency shift and areal mass density. Data were acquired through a combined QCM-D and spectroscopic ellipsometry (SE; M2000V, J. A. Woollam, Lincoln, NE, USA) measurement. The graph shows Δf (from QCM-D) vs. areal mass density Γ (from SE) for the adsorption under static conditions of **3** (A, blue line; at a total HS concentration of 1 $\mu\text{g}/\text{mL}$), and of a biotinylated oligonucleotide (B, green line; at 1.56 $\mu\text{g}/\text{mL}$) that served as a reference molecule in Fig. S5. The data are well approximated by straight lines through the origin (black lines) confirming that the relationship between Δf and Γ is roughly linear for these compounds. The slopes of the linear fits $\Delta f/\Delta\Gamma$ were -0.67 ± 0.01 Hz/(ng/cm²) for **3** and -0.42 ± 0.01 Hz/(ng/cm²) for the biotinylated oligonucleotide (mean \pm S.E.M. from three independent measurements). The combined QCM-D and SE measurement was performed with a custom-built open fluid cell as described earlier.^{4, 5} Before use, the walls of the fluid cell were passivated against biomolecular binding with BSA. SE measures changes in the polarization of light upon reflection at a planar surface, from which the areal mass density can be quantified through fitting of the SE data to an optical model. Fitting was performed, as described in detail elsewhere;⁶ the opaque gold film with the OEG monolayer was treated as a single isotropic layer and fitted as a B-spline substrate; SA_v and b-HS film were considered as separate transparent Cauchy layers; b-HS areal mass densities were determined through de Fejter's equation,⁴ using a refractive index increment of $dn/dc = 0.15$ cm³/g.

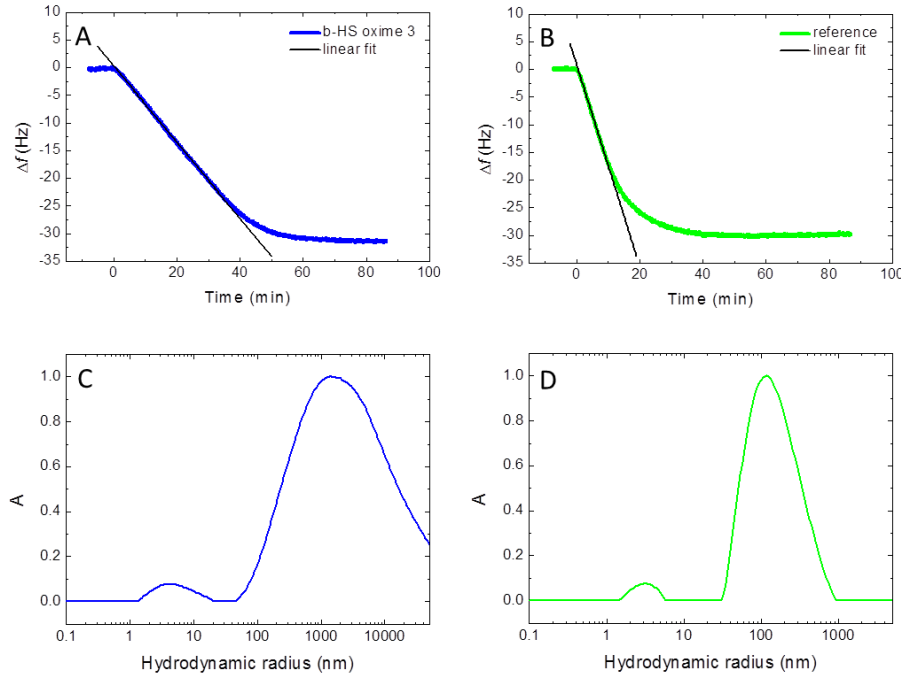


Figure S5. Quantification of active analyte concentrations from QCM-D binding assays. (A-B) QCM-D responses (Δf) for the adsorption of **3** (freshly defrozen and incubated at 1 $\mu\text{g/mL}$ total HS concentration; A) and a biotinylated oligonucleotide (incubated at $c_{\text{ref}} = 1.56 \mu\text{g/mL}$; B) to a SAV monolayer. The oligonucleotide served as reference molecule to determine the concentration of intact b-HS, $c_{\text{b-HS}}$, in the HS solution, as described in the following. Binding of an analyte (b-HS in our case) to a ligand (SAV) on the QCM-D sensor surface is a two-step event, consisting of mass transfer to the sensor surface followed by the actual binding to the ligand. Since the biotin-SAV bond forms rapidly, the first step is rate limiting in our assay, except at high coverage where the scarcity of available binding sites limits binding. For mass-transfer limited binding, the binding rate depends exclusively on the flow conditions (i.e. flow-cell geometry and flow rate, maintained constant in our assay) and the analyte's active concentration (i.e. the concentration of HS being effectively biotin-conjugated, $c_{\text{b-HS}}$) and diffusion coefficient, $D_{\text{b-HS}}$.⁷ Considering the flow conditions in our experimental setup (i.e. laminar flow in a slit), the binding rate is given by

$$\left. \frac{\Delta\Gamma}{\Delta t} \right|_{\text{b-HS}} \propto D_{\text{b-HS}}^{2/3} c_{\text{b-HS}} \quad [\text{Eq. S1}]$$

in steady state.⁷ From a comparative measurement with a reference molecule of known concentration c_{ref} and diffusion coefficient D_{ref} , the analyte's active concentration can be determined through

$$c_{\text{b-HS}} = c_{\text{ref}} \left(\frac{D_{\text{ref}}}{D_{\text{b-HS}}} \right)^{2/3} \frac{\left. \frac{\Delta\Gamma}{\Delta t} \right|_{\text{b-HS}}}{\left. \frac{\Delta\Gamma}{\Delta t} \right|_{\text{ref}}} \quad [\text{Eq. S2A}]$$

The ratio $D_{\text{ref}}/D_{\text{b-HS}}$ is identical to the ratio of the molecules' hydrodynamic radii $r_{\text{h,b-HS}}/r_{\text{h,ref}}$ due to the Stokes-Einstein equation. Moreover, the relationship between Γ and Δf is linear for the molecules of interest (Fig. S4), and hence

$$c_{\text{b-HS}} = c_{\text{ref}} \left(\frac{r_{\text{h,b-HS}}}{r_{\text{h,ref}}} \right)^{2/3} \left(\frac{\left. \frac{\Delta f}{\Delta t} \right|_{\text{b-HS}}}{\left. \frac{\Delta f}{\Delta t} \right|_{\text{ref}}} \right) \left(\frac{\left. \frac{\Delta\Gamma}{\Delta t} \right|_{\text{ref}}}{\left. \frac{\Delta\Gamma}{\Delta t} \right|_{\text{b-HS}}} \right) \quad [\text{Eq. S2B}]$$

The extended linear binding regimes in A and B (black solid lines are fits with slopes $\Delta f/\Delta t|_{\text{b-HS}} = -0.82 \pm 0.03 \text{ Hz/min}$ and $\Delta f/\Delta t|_{\text{ref}} = -1.86 \pm 0.03 \text{ Hz/min}$ (mean \pm S.E.M. from three independent measurements)) confirm mass-transfer limited binding in steady state. Equation S2B, with $\Delta f/\Delta\Gamma$ taken from Fig. S4 and r_{h} determined through dynamic light scattering (see C-D below), resulted in $c_{\text{b-HS}} = 0.54 \pm 0.08 \mu\text{g/mL}$. Finally, comparison with the total HS concentration employed reveals that $54 \pm 8\%$ of the HS chains were effectively biotinylated. This value is in excellent agreement with the yield obtained through weighing of purified HA_dp4 **10** (Fig. S1).

Equation S1 shows that, during mass-transfer limited binding, the binding rate is directly proportional to the analyte's active concentration, and a reduction in the binding rate (e.g. in Fig. 1) reflects a proportional decrease in the analyte's active concentration (since the analyte's diffusion coefficient is unchanged). To obtain the fractions of b-HS in Fig. 2, relative changes in the slopes in Fig. 1 were compared, and combined with the value of 54% for freshly defrozen **3**.

(C-D) Quantification of hydrodynamic radii by dynamic light scattering (DLS). Mass-weighted distributions (A) of hydrodynamic radii (r_{h}) of HS_12kDa **1** (C) and the reference oligonucleotide (D) with peaks at $r_{\text{h,b-HS}} = 4.7 \pm 0.2 \text{ nm}$ and $r_{\text{h,ref}} = 3.3 \pm 0.1 \text{ nm}$ (mean \pm S.E.M. from 6 independent measurements; we estimate that addition of the small biotin moiety to polymeric HS and oligonucleotide does not affect r_{h} appreciably) corresponding to the size of individual molecules. Secondary peaks at 100 nm and more are likely to correspond to aggregates; although these peaks dominate the mass-weighted distribution, their contribution in numbers is very small (less than 0.1%). Measurements were performed as described in detail elsewhere.⁸ Autocorrelation functions were collected at $25.0 \pm 0.1 \text{ }^\circ\text{C}$ for a counting time of 60 s at 90 degrees scattering angle. Radius distributions were obtained using CONTIN analysis⁹ of the autocorrelation functions.

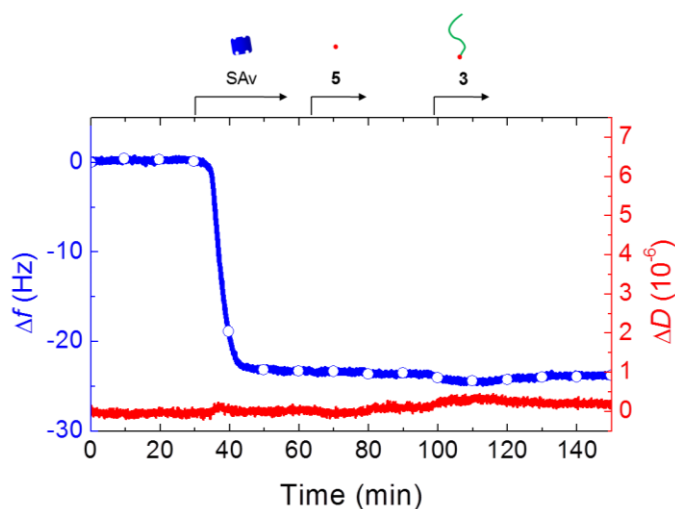


Figure S6. Binding of free biotin to streptavidin monolayers does not elicit a measurable QCM-D response. QCM-D responses (Δf – blue lines with circle symbols, ΔD – red lines) during the formation of a SAV monolayer (conditions as in Fig. S3) followed by sequential exposure to b-OEG-ONH₂ **5** (50 $\mu\text{g}/\text{mL}$) and **3** (50 $\mu\text{g}/\text{mL}$). Start and duration of sample incubation steps are indicated by arrows on top of the plot; during remaining times, the surface was exposed to Hepes buffer solution. The absence of b-HS binding confirms that free biotin saturated all biotin-binding sites on the SAV monolayer. Yet, the SAV-bound biotin (i.e. **5**) did not by itself give rise to a measurable QCM-D response, presumably due to the compound's low molecular weight and the location of the biotin-binding pocket deep inside SAV.

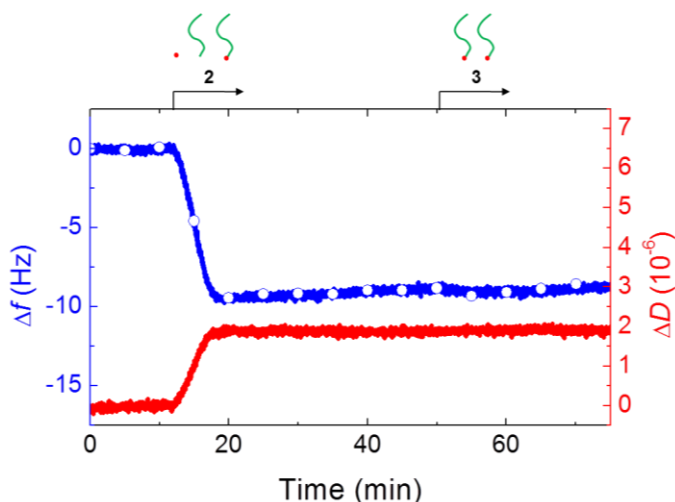


Figure S7. Free biotin, released upon degradation, contributes to the occupation of binding sites in streptavidin monolayers. QCM-D responses (Δf – blue lines with circle symbols, ΔD – red lines) during the adsorption of a partially degraded sample (**2**, 7 days storage at 4°C; 50 $\mu\text{g}/\text{mL}$) to a SAV monolayer followed by incubation of a non-degraded sample (**3**, freshly de-frozen; 50 $\mu\text{g}/\text{mL}$). Start and duration of sample incubation steps are indicated by arrows on top of the plot; during remaining times, the surface was exposed to Hepes buffer solution. Incubation with the non-degraded sample did not lead to significant additional binding. This confirms that no free biotin binding sites were available after incubation with the supposedly degraded sample, i.e. the biotin released due to degradation saturates all available biotin binding pockets.

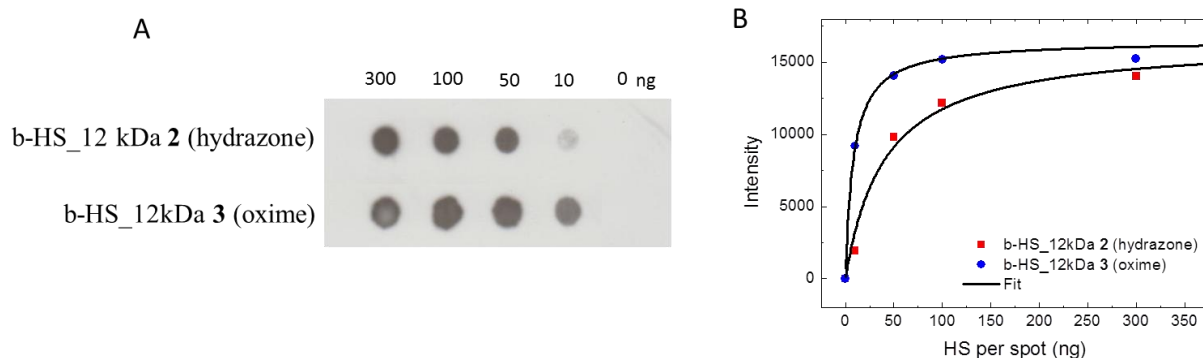


Figure S8. Dot-blot analysis confirms HS biotinylation. 50 μ L of b-HS samples at a range of total HS concentrations were spotted on a (positively charged) nitrocellulose membrane (Genomic Zeta-Probe; Bio-Rad, Marnes-la-Coquette, France) which retains (negatively charged) HS but not free biotin. Membranes were pre-washed with PBS at pH 7.4 using a vacuum-assisted dot-blot apparatus, rinsed twice with PBS, blocked for 30 min at 37°C in a 5% (w/v) dry milk solution in Tris-buffered saline (TBS; Sigma-Aldrich) at pH 7.4, and extensively rinsed with TBS. The blots were probed with extravidin-labeled horseradish peroxidase (exAvHRP; Sigma-Aldrich) diluted 1:3000 in TBS with 0.05% (w/v) Tween20 for 45 min under shaking. After 6 cycles of washing (5 min each) with TBS and 0.05% (w/v) Tween20 at RT, the biotinylated samples were revealed by incubation of the membrane with hydrogen peroxide and the chemiluminescent detection reagent (Luminata Classico Western HRP Substrate; Millipore, Molsheim, France) for 1 min, followed by autoradiography (Amersham Hyperfilm ECL; GE Healthcare). (A) Autoradiograph of membranes spotted with **2** and **3** with total HS quantities per spot (in ng) indicated. (B) Dot intensities, quantified by densitometry using ImageJ software, for b-HS hydrazone **2** (red squares) and b-HS oxime (blue circles) from the membrane displayed in A. Intensities were offset by the intensity of the control samples lacking b-HS (0 ng). Both data sets were well approximated by the expression $I = I_{\max}[\text{HS}]/([\text{HS}] + [\text{HS}]_{1/2})$, where I_{\max} is the intensity at saturation, $[\text{HS}]$ the total HS quantity per spot and $[\text{HS}]_{1/2}$ the total HS quantity at which half-maximal intensity is attained. Black lines are best fits, giving $I_{\max} = 16500$ (set to be identical for both curves) and $[\text{HS}]_{1/2} = 40.6$ and 8.3 ng for **2** and **3**, respectively. The ratio of the two $[\text{HS}]_{1/2}$ values is 4.9, confirming that the concentration of biotinylated HS in the oxime conjugate **3** is about 5 times larger than in the equivalent hydrazone conjugate **2**, as determined from the analysis of the QCM-D data (Figs. 2 and S5).

Supplementary References

1. B. Mulloy, C. Gee, S. F. Wheeler, R. Wait, E. Gray and T. W. Barrowcliffe, *Thromb. Haemost.*, 1997, **77**, 668–674.
2. E. Saesen, S. Sarrazin, C. Laguri, R. Sadir, D. Maurin, A. Thomas, A. Imberty and H. Lortat-Jacob, *J. Am. Chem. Soc.*, 2013, **135**, 9384–9390.
3. A. Amara, O. Lorthioir, A. Valenzuela, A. Magerus, M. Thelen, M. Montes, J.-L. Virelizier, M. Delepierre, F. Baleux, H. Lortat-Jacob and F. Arenzana-Seisdedos, *J. Biol. Chem.*, 1999, **274**, 23916–23925.
4. R. P. Richter, K. B. Rodenhausen, N. B. Eisele and M. Schubert, in *Ellipsometry of Functional Organic Surfaces and Films*, Springer Series in Surface Sciences, 2014, vol. 52, pp. 223–248.
5. I. Carton, A. R. Brisson and R. P. Richter, *Anal. Chem.*, 2010, **82**, 9275–9281.
6. G. V. Dubacheva, T. Curk, B. M. Mognetti, R. Auzely-Velty, D. Frenkel and R. P. Richter, *J. Am. Chem. Soc.*, 2014, **136**, 1722–1725.
7. W. T. Hermens, M. Benes, R. Richter and H. Speijer, *Biotechnol. Appl. Biochem.*, 2004, **39**, 277–284.
8. C. Travelet, M. Stemmelen, V. Lapinte, F. Dubreuil, J.-J. Robin and R. Borsali, *J. Nanopart. Res.*, 2013, **15**.
9. J. Bodycomb and M. Hara, *Macromolecules*, 1995, **28**, 8190–8197.